

Simple Lattice Simulation of Chiral Discrimination in Monolayers

Linyong Mao, Harold H. Harris, and Keith J. Stine*

Department of Chemistry and Biochemistry, University of Missouri–St. Louis, St. Louis, Missouri 63121

Received April 19, 2002

A simulation method based on cellular automata on a hexagonal lattice is applied to model the behavior of chiral molecules on a surface, such as those in a monolayer of amphiphiles each having a single chiral center. The simulation method includes movement and orientation rules, with the objects (“molecules”) on the lattice vertices possessing three different groups with one group pointing along each edge. Periodic boundary conditions are employed in the simulations. Interaction strengths are calculated between pairs of groups occupying the edges between vertices and summed for the entire system. The model successfully reproduces the formation of domains as a consequence of the movement rule. The movement rule can be adjusted to simulate homochiral discrimination or heterochiral discrimination for the case of racemic mixtures. The orientation rule results in a preference for orientations of the molecules that minimize the total interaction strength.

INTRODUCTION

Chirality is an aspect of many phenomena in chemistry and biology, playing a key role in the assembly of supramolecular structures and in recognition events between biomolecules. Monolayers at the water–air interface are an example of a physical system where the effects of chirality can be studied in two-dimensions.¹ Monolayers have been studied for decades,² with the field receiving renewed attention over the past two decades due to the availability of new methods for characterizing these systems.³ Among these methods, fluorescence microscopy⁴ and Brewster angle microscopy⁵ have allowed for the direct observation of monolayer microstructure at the water–air interface. The classical method of characterizing monolayer phase behavior by the measurement of surface pressure (Π) versus mean molecular area (A) isotherms clearly shows the occurrence of first-order phase transitions with two-phase coexistence regions.^{6,7} The most commonly encountered coexistence regions in monolayer phase diagrams are those between the two-dimensional gas phase (G) and the liquid-expanded phase (LE), between the LE phase and the liquid-condensed phase (LC), or between the gas phase and the LC phase. In these coexistence regions, microscopy observations show a variety of microstructures consisting of domains of the coexisting phases that are typically in the microns size range; often one observes islands of one of the two phases surrounded by the other phase.^{8–10}

Studies of the effect of chirality on the behavior of monolayers at the water–air interface have often focused on comparing the behavior of films of a single enantiomer with those of a racemic mixture.¹¹ If the amphiphiles studied have one chiral center and chiral discrimination occurs, then it can be described as either homochiral discrimination or heterochiral discrimination. In the case of homochiral discrimination, there is a preferential interaction between like

enantiomers; heterochiral discrimination occurs when there is a preferential interaction between opposite enantiomers. In the case of homochiral discrimination, monolayers of the enantiomer are more “condensed” than those of racemic mixture, having smaller limiting mean molecular areas due to closer molecular packing. The reverse situation holds for the case of heterochiral discrimination; monolayers of the enantiomer are more “expanded” than monolayers of a racemic mixture. A number of studies have concerned the behavior of amphiphiles with amino acid headgroups.^{12–21,23,34} Chiral discrimination in monolayers results in differences in Π - A isotherms, in domain microstructures,^{12–17,34} and in vibrational spectra.^{18,19} In some microscopy studies, chiral domain shapes were observed and evidence for chiral segregation in racemic films showing homochiral discrimination was found, and this was also seen in grazing incidence X-ray diffraction experiments.^{20,21} Scanning force microscopy studies on transferred films showed molecular scale differences in lattice structures.^{22,23}

The present study concerns the development of a lattice model inspired by cellular automata^{24,25} and its application to reproducing the general features observed in the behavior of monolayers of chiral molecules. Cellular automata simulations represent a complex system as an array of cells (automatons) whose states evolve discretely subject to intuitive and easily stated local rules. In these simulations, patterns and phenomena like those of the physical system represented emerge starting from random state configurations after some number of iteration cycles based on the rules. An advantage of cellular automata simulations is the prospect of efficiently representing phenomena that would be difficult to model using traditional simulation methods and perhaps impossible to model analytically. The application of cellular automata to physical systems has become an area of growing interest and has been surveyed in a recent text.²⁶ Applications of cellular automata to aqueous systems have been reviewed.²⁷ A cellular automata model was found to success-

*Corresponding author phone: (314)516-5346; fax: (314)516-5342; e-mail: kstine@jinx.ums1.edu.

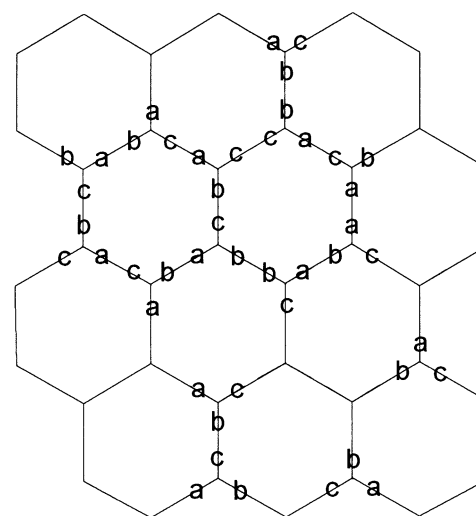
fully generate the chiral structure induced in the water molecules surrounding a chiral solute molecule.²⁸

In the model presented in this paper, each occupied cell of a two-dimensional hexagonal grid represents a chiral molecule that responds to the state of its neighboring cells according to simple rules. The entire system evolves in a sequence of steps during which each molecule has a chance to change its orientational state and/or move. Simulations using the presented model produce island structures resembling the domains observed in microscopy studies of monolayers, and the model can be adjusted to produce behavior consistent with either homochiral or heterochiral discrimination.

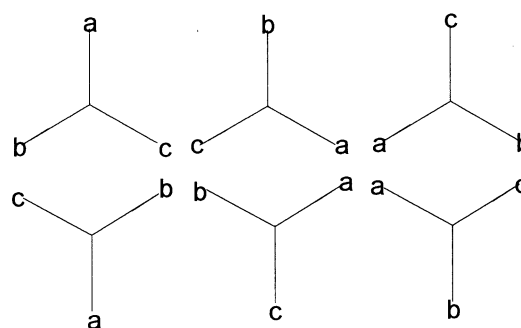
METHODS

Figure 1a shows a hexagonal model where the hexagonal vertices are either empty or occupied by a "molecule" with one chiral center. In Figure 1, "a", "b", and "c" represent three constituents of a chiral molecule. The order of a, b, and c is always counterclockwise in the figure, representing a monolayer of a single enantiomer. A fourth "constituent" could be imagined to point away from the plane, and while not present in the simulation it could be thought of as the alkyl chain. The representation is inspired by Andelman's tripod amphiphile model.^{29–31} The constituents may be assigned full or partial charges, and the interaction strength between a pair of constituents oriented facing each other on an edge between two occupied sites can be calculated as the product of the assigned charges. Only molecules on sites connected by an edge of the hexagonal lattice are considered to be neighbors. For empty sites, a, b, and c are all assigned a value of zero. In the simulations presented, $a = +1$, $b = -1$, and $c = 0.1$. The equal and opposite values assigned to constituents a and b could be thought of as representing a zwitterionic headgroup or two complimentary groups such as a hydrogen-bond acceptor and a hydrogen-bond donor. The group c could be a smaller group such as a hydrogen atom. For a given chiral molecule, there are six different possible orientations on a hexagonal grid as represented in Figure 1b. To display these orientations, six different colors were used with empty sites represented by the color white. The orientations and the colors used are shown in Figure 1c. To distinguish between "D" and "L" enantiomers, circles are used to represent the L enantiomers and squares are used to represent the D enantiomers. For the L enantiomers, a, b, and c are arranged in a counterclockwise sequence; while for the D enantiomers, a, b, and c are arranged in a clockwise sequence.

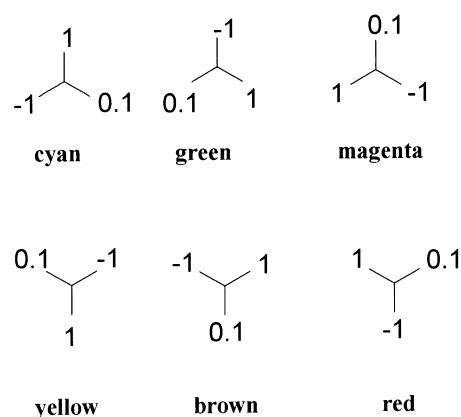
The sum of all interaction strengths between pairs of neighboring constituents is defined to be the total interaction strength (TIS). The sum of the number of molecules neighboring each molecule is defined as the total aggregation number (TAN). If a molecule is located on a site such that a single constituent points up (magenta, cyan, or green), and the molecule above it is of the orientation denoted by the color brown, then the most favorable orientation will be that represented as magenta. The orientation of a molecule with one constituent pointing up is only determined by the orientation of the molecule above it. If this site is empty, then the molecule can adopt any one of the three possible orientations. If a molecule with a single constituent pointing



(A)



(B)



(C)

Figure 1. (a) Illustration of the hexagonal model used in these simulations, the letters a, b, and c represent the three constituents of a chiral molecule occupying the site. (b) The six different orientations of a chiral molecule on the hexagonal lattice. (c) The colors used in the simulation output to represent each orientation and the values assigned to the constituents for the purpose of determining interaction strengths ($a = +1$, $b = -1$, $c = 0.1$).

up is cyan, then the most favorable orientation for the one above it will be red. A molecule in the orientation represented by green pointing up will result in the above molecule preferring the orientation represented by yellow. For molecules on the sites where one constituent points down, the orientation is determined so that the interaction strength between the molecule and the two neighbors above it is the most negative.

The molecules are allowed to move at each step of the simulation to an unoccupied site. The molecules can also reorient and thus will change color. In the simulation, a defined number of molecules are initially randomly distributed on the hexagonal lattice. The positions and orientations are then allowed to evolve in cycles. During each cycle, the status of a molecule is first evaluated according to a movement rule. The molecules on the hexagonal lattice are subject to periodic boundary conditions so that if they move off an edge they return on the opposite edge. The movement rule applied does not allow a molecule to move if it has two neighbors, it is allowed to move if it has a neighbor or no neighbors and cannot move if it is surrounded. If it is allowed to move, then it will do so with each available direction and the possibility of not moving being equally probable. After all of the movements, reorientation is allowed according to the orientation rule. The orientation rule places a molecule in the orientation such that the interaction strength with its neighboring molecules is the most negative. At the end of each cycle, the values of TIS and TAN are calculated for the entire system. After thousands of cycles, characteristic patterns emerge, and the values of TIS and TAN stabilize.

To simulate racemic mixtures, the movement rule is modified depending on whether the homochiral or heterochiral case is being simulated. For the homochiral case, the movement rule is modified so that a molecule will not move if it has two neighbors of the same chirality. For the heterochiral case, the movement rule is modified so that a molecule will not move if it has two neighbors of opposite chirality. In the simulations of racemic mixtures, the total discrimination number (TDN) is introduced as variable to be calculated after each cycle. A lattice edge connecting two like enantiomers contributes +1 to the value of TDN, and a lattice edge connecting two opposite enantiomers contributes -1 to the value of TDN.

The code for the simulation was written by the authors in Borland C++ (version 5.0) and run on a PC under Windows 98; it is available from the authors by request.

RESULTS

Figure 2 shows the configuration of 640 molecules on an 80×40 grid after 20 000 cycles of evolution. Clustering of the molecules into islands of different sizes is clearly seen, along with some isolated molecules and small clusters. Figure 3a shows the variation of the total aggregation number (TAN) versus cycle number, and Figure 3b shows the variation of the total interaction strength (TIS) versus cycle number. The plot of TAN versus cycle number shows that aggregation occurs rapidly in the early steps and progressively slows as the steady state is reached. It can be seen that these parameters fluctuate as they asymptotically approach stable values. The limiting value of TAN (near 1618) divided by the number of molecules (640) gives an average number of

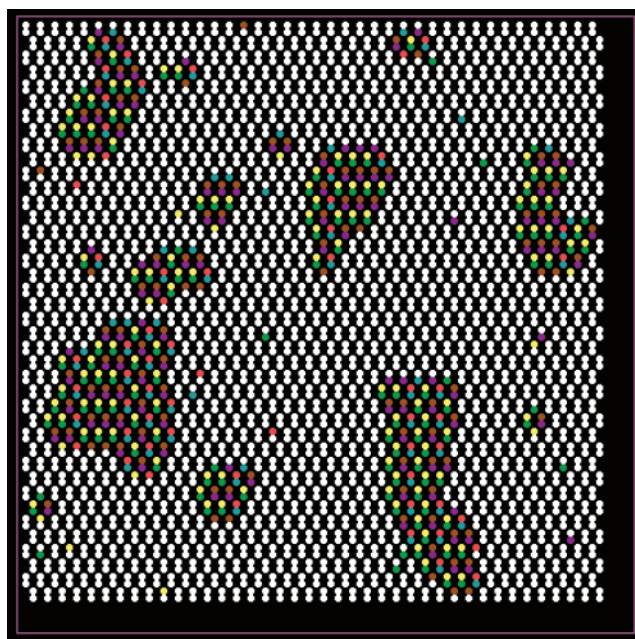


Figure 2. The configuration of 640 chiral molecules of the same enantiomer (L form) on an 80×40 hexagonal grid after 20 000 cycles of evolution. The depiction of the simulation output is color coded as noted in Figure 1.

neighbors per molecule of 2.5. The ideal minimum value for the TIS for 640 molecules would be -636.8 ($(-1.99 \times 640)/2$) neglecting edge effects. The value of TIS observed near the end of the simulation is near -476 , which is about 75% of the ideal minimum value. It appears that TIS fluctuates more than TAN during the simulation.

Figure 4 shows the configuration of 1600 molecules on an 80×40 grid after 4000 cycles. There are interconnections between islands and more extended shapes. It was found that the larger number of molecules required fewer cycles to reach a stable configuration due to the smaller number of movement cycles required for a molecule to encounter two neighbors. The values of TAN and TIS reached steady-state values well within 2000 cycles. The average number of neighbors per molecule attained was 2.5, and the value of TIS reached was about 74% of the ideal minimum.

Figure 5 shows the configuration of 640 molecules, where 320 are of the D form (circles) and 320 are of the L form (boxes), after 40 000 cycles of evolution on the 80×40 grid. In this simulation, the movement rule modified to promote homochiral discrimination was used. The formation of islands is evident, and there is a tendency for the islands to be composed of either circles or boxes. The formation of separate islands composed of circles or boxes represents chiral segregation in this model. The separation is not perfect as seen in the island in the lower left.

Figure 6 shows the configuration of 1600 molecules, 800 of the D form (circles) and 800 of the L form (boxes), on an 80×40 grid after 4000 cycles. In this simulation, the movement rule modified to promote heterochiral discrimination was used. The formation of extended islands is evident, and it can be seen that squares prefer to neighbor circles. This represents the case of heterochiral discrimination with opposite enantiomers preferring to neighbor each other in the structure.

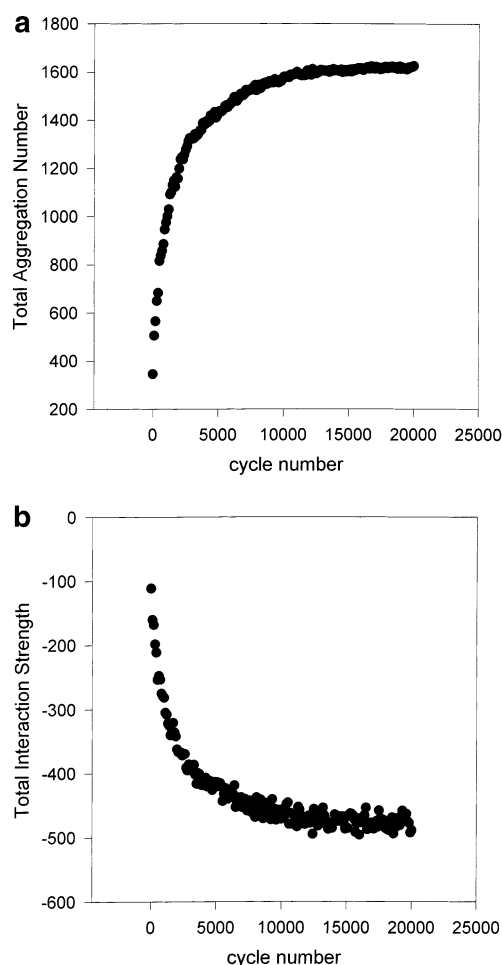


Figure 3. (a) The evolution of the total aggregation number (TAN) versus cycle number for the simulation shown in Figure 2. (b) The evolution of the total interaction strength (TIS) versus cycle number for the simulation shown in Figure 2. The points are plotted at 100 cycle intervals.

The rate of evolution of the values of TAN and TIS are different for the case of a single enantiomer, the case of a racemic mixture with homochiral discrimination, and the case of a racemic mixture with heterochiral discrimination, as can be seen in Figure 7. For the same number of molecules, the case of one enantiomer alone approaches a steady state more quickly than either the heterochiral or especially the homochiral case. This is seen clearly in the plot of TAN versus cycle number (Figure 7a) and in the plot of TIS versus cycle number (Figure 7b). It is to be expected that the homochiral case will approach a steady state more slowly given the additional movement required in order to attain a segregation of opposite enantiomers. The evolution of the total discrimination number (TDN) is different for the cases of homochiral and heterochiral discrimination. The value of TDN starts near zero and then increases for the homochiral model. For the heterochiral model, it starts near zero and decreases consistent with its definition and the evolution of the system according to the modified movement rule.

DISCUSSION

The simulation method used here, while simple, generated configurations possessing many of the key features observed in monolayers of chiral molecules undergoing aggregation

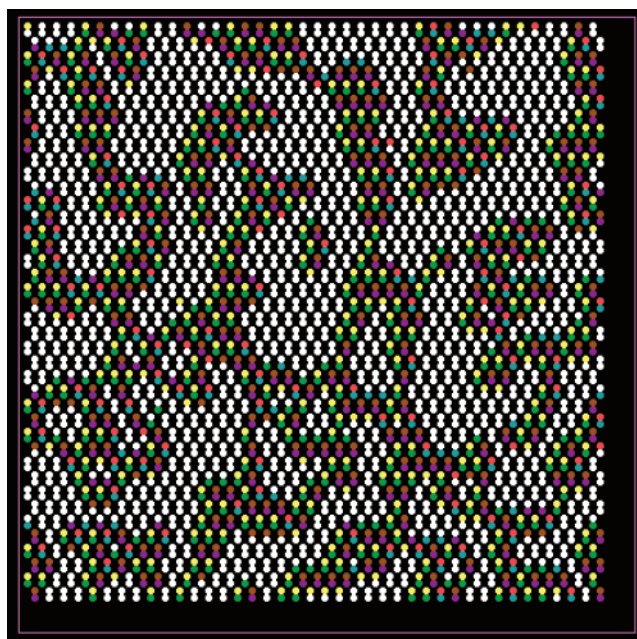


Figure 4. The configuration of 1600 chiral molecules of the same enantiomer (L form) on an 80×40 hexagonal grid after 4000 cycles of evolution. The depiction of the simulation output is color coded as noted in Figure 1.

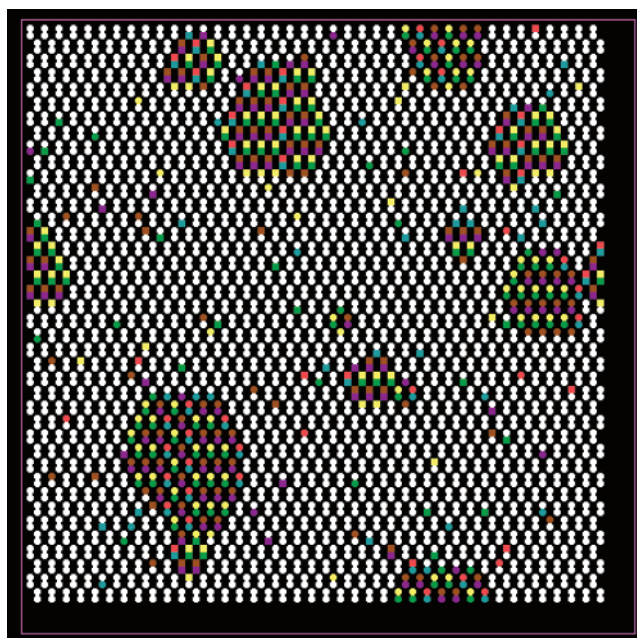


Figure 5. The configuration of 640 chiral molecules on an 80×40 hexagonal grid. The 640 molecules consist of 320 L enantiomers (circles) and 320 D enantiomers (squares). The simulation used the movement rule modified to yield homochiral discrimination.

on a water surface. Given that there are occupied sites and unoccupied sites in the model, the region of the monolayer phase diagram most represented by the model would be the liquid-condensed + gas-phase coexistence region.⁷ At temperatures below where there is a liquid-expanded phase, the monolayer appears as islands of condensed phase surrounded by a two-dimensional gas phase which is of very low surface density.^{7,15} A morphology having some similarity to the interconnected pattern in Figure 4 has been observed in the liquid-condensed + liquid-expanded coexistence region of monolayers of octadecylamine on an acidified subphase.³²

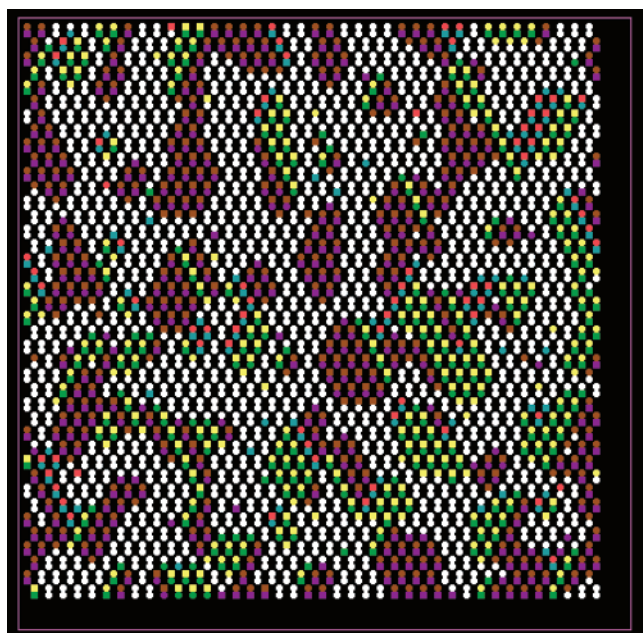


Figure 6. The configuration of 1600 chiral molecules on an 80×40 hexagonal grid. The 1600 molecules consist of 800 L enantiomers (circles) and 800 D enantiomers (squares). The simulation used the movement rule modified to yield heterochiral discrimination.

Interconnected foamlike patterns are common in the liquid-expanded + gas coexistence region.⁷

The appearance of separated domains of the two enantiomers in Figure 5 is consistent with observations using scanning probe microscopy of separated regions of mirror image lattice structures in Langmuir–Blodgett (LB) films of racemic mixtures of a tetracyclic alcohol²² and in LB films of racemic mixtures of N-stearoylglutamic acid.²³ N-stearoylglutamic acid, being an N-acyl amino acid with one chiral center, is the kind of molecular structure represented by the tripod amphiphile model and in the present simulations. X-ray diffraction data on racemic N-myristoylalanine monolayers showing homochiral discrimination revealed an oblique lattice structure consistent with regions of separated enantiomers.²⁰ Separation of enantiomers in racemic monolayers of N-stearoylserine methyl ester¹⁵ and of N-stearoylvaline¹⁷ was inferred from domain shapes by fluorescence microscopy. Thus, the simulations have successfully generated separation of enantiomers in a racemic monolayer for the case of homochiral discrimination. A feature of the domains observed by microscopy not reproduced by the model in its present form is that of domain curvature of a sense uniquely determined by the molecular chirality. Curved domains have been observed for racemic monolayers subject to homochiral discrimination and for monolayers of pure enantiomers but not for all systems.^{15–17} Curved domains were observed for the liquid-condensed phase of N-stearoylserine methyl ester in the liquid-condensed + liquid-expanded coexistence region but not in the lower temperature liquid-condensed + gas coexistence region.¹⁵ Curved domains were not observed for enantiomeric films of N-stearoylvaline but were observed for the racemic monolayer.¹⁷ However, there is no reason to expect the model in its present form to produce curved domain shapes.

The appearance of the domains of the racemic mixture of enantiomers subject to heterochiral discrimination shown in

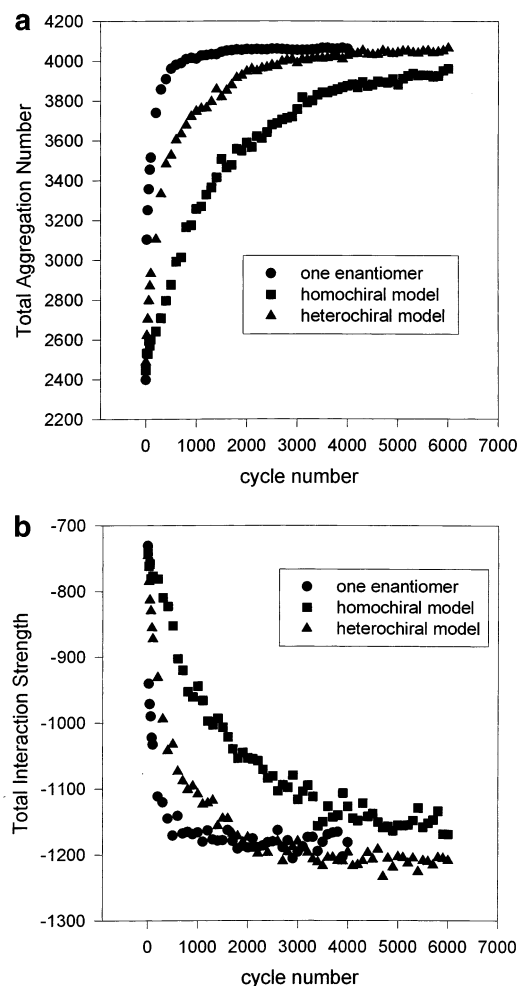


Figure 7. (a) Total aggregation number (TAN) versus cycle number for 1600 molecules on an 80×40 hexagonal grid and the cases of one enantiomer (circles), the heterochiral discrimination case (triangles), and the homochiral discrimination case (squares). (b) Total interaction strength (TIS) versus cycle number for 1600 molecules on an 80×40 hexagonal grid and the cases of one enantiomer (circles), the heterochiral discrimination case (triangles), and the homochiral discrimination case (squares). The simulation output values are plotted at 100 cycle intervals.

Figure 6 is similar to what one might expect for the case of racemate formation, which has been observed most definitively in 2-heptadecanol monolayers.³³ In Figure 6, it can be seen that the opposite enantiomers (squares and circles) associate with each other regularly and with consistently matched orientations with a small number of exceptions visible in the pattern. A racemate represents a highly ordered association between opposite enantiomers, in contrast to the case of a solid solution for which the two enantiomers would be more randomly mixed. Whether or not a racemate or solid solution form appears to depend on the strength of the chiral interactions, it was observed experimentally that 2-hexadecanol formed solid solutions while racemate formation was observed in monolayers of 2-heptadecanol.³³ Thus, the simulation has demonstrated heterochiral discrimination corresponding to the case of racemate formation.

To include a population of automaton sites representing a liquid-expanded phase, a fraction of the sites not occupied by a liquid-condensed phase molecule could be filled to represent a lower density liquid-expanded phase for which the values of the constituents are smaller and equal to

represent free molecular rotation. Setting the fraction of sites unfilled high enough to still allow movement on the lattice would allow simulations representing the liquid-condensed + liquid-expanded coexistence to be attempted. Variation of the relative values of the constituents and of the movement and orientation rules would allow for other situations to be explored, such as mixtures of two different chiral molecules or mixtures of chiral molecules with achiral molecules.³⁴ Simulations using models similar to that presented here may also be applicable to the adsorption of chiral molecules on clays³⁵ or on faces of single crystals.³⁶ Simulations of adsorption of chiral molecules onto a surface would involve adding molecules at random sites during the iterations. These ideas remain as interesting avenues for further investigation.

REFERENCES AND NOTES

- (1) Arnett, E. M.; Harvey, N. G.; Rose, P. L. Stereochemistry and Molecular Recognition in "Two Dimensions". *Acc. Chem. Res.* **1989**, *22*, 131–138.
- (2) Gaines, G. L. *Insoluble Monolayers at Liquid–Gas Interfaces*; John Wiley and Sons: New York, 1966.
- (3) Petty, M. C. *Langmuir–Blodgett Films: An Introduction*; Cambridge University Press: Cambridge, UK, 1996.
- (4) Stine, K. J. Fluorescence Microscopy for Studying Biological Model Systems: Phospholipid Monolayers and Chiral Discrimination Effects. In *Physical Chemistry of Biological Interfaces*; Baskin, A., Norde, W., Eds.; Marcel Dekker: New York, 1999; Chapter 22, p 749.
- (5) Lheveder, C.; Hénon, S.; Meunier, J. Brewster Angle Microscopy. In *Physical Chemistry of Biological Interfaces*; Baskin, A., Norde, W., Eds.; Marcel Dekker: New York, 1999; Chapter 16, p 559.
- (6) Knobler, C. M. Recent Developments in the Study of Monolayers at the Air–Water Interface. In *Advances in Chemical Physics*; Prigogine, I., Rice, S. A., Eds.; John Wiley and Sons: New York, 1990; Vol. 77, p 387.
- (7) Moore, B.; Knobler, C. M.; Akamatsu, S.; Rondelez, F. Phase Diagram of Langmuir Monolayers of Pentadecanoic Acids: Quantitative Comparison of Surface Pressure and Fluorescence Microscopy Results. *J. Phys. Chem.* **1990**, *94*, 4588–4595.
- (8) McConnell, H. M. Structures and Transitions in Lipid Monolayers at the Air–Water Interface. In *Annual Reviews of Physical Chemistry*; Annual Reviews: Palo Alto, 1991; Vol. 42, p 171.
- (9) Stine, K. J.; Knobler, C. M. Fluorescence Microscopy: A Tool for Studying the Physical Chemistry of Interfaces. *Ultramicroscopy* **1992**, *47*, 23–34.
- (10) Stine, K. J. Investigations of Monolayers by Fluorescence Microscopy. *Microscopy Res. Technique* **1994**, *27*, 439–450.
- (11) Stine, K. J. Chirality in Monolayers. In *Encyclopedia of Surface and Colloid Science*; Hubbard, A. T., Ed.; Marcel Dekker: New York, 2002; p 1017.
- (12) Marr-Leisy, D.; Neumann, R.; Ringsdorf, H. The Comparative Spreading Behavior of Enantiomeric and Racemic Tyrosine Amphiphiles. *Coll. Polym. Sci.* **1985**, *263*, 791–798.
- (13) Bouloussa, O.; Dupeyrat, M. Chiral Discrimination in N–Tetradecanoylalanine and N–Tetradecanoylalanine/Ditetradecanoylphosphatidylcholine Monolayers. *Biochim. Biophys. Acta* **1988**, *938*, 395–402.
- (14) Harvey, N. G.; Mirajovsky, D.; Rose, P. L.; Verbiar, R.; Arnett, E. M. Molecular Recognition in Chiral Monolayers of Stearoylserine Methyl Ester. *J. Am. Chem. Soc.* **1989**, *111*, 1115–1122.
- (15) Stine, K. J.; Uang, J. Y.-J.; Dingman, S. D. Comparison of Enantiomeric and Racemic Monolayers of N–Stearoylserine Methyl Ester by Fluorescence Microscopy. *Langmuir* **1993**, *9*, 2112–2118.
- (16) Stine, K. J.; Whitt, S. A.; Uang, J. Y.-J. Fluorescence Microscopy Study of Langmuir Monolayers of Racemic and Enantiomeric N–Stearoyltyrosine. *Chem. Phys. Lipids* **1994**, *69*, 41–50.
- (17) Parazak, D. P.; Uang, J. Y.-J.; Turner, B.; Stine, K. J. Fluorescence Microscopy Study of Chiral Discrimination in Langmuir Monolayers of N–Acylvaline and N–Acylalanine Amphiphiles. *Langmuir* **1994**, *10*, 3787–3793.
- (18) Gericke, A.; Hühnerfuss, H. Infrared Comparison of Enantiomeric and Racemic N–Octadecylserine Methyl Ester Monolayers at the Air/Water Interface. *Langmuir* **1994**, *10*, 3782–3786.
- (19) Hoffmann, F.; Hühnerfuss, H.; Stine, K. J. Temperature Dependence of Chiral Discrimination in Langmuir Monolayers of N–Acyl Amino as Inferred from Π/A Measurements and Infrared Reflection–Absorption Spectroscopy. *Langmuir* **1998**, *14*, 4525–4534.
- (20) Nassoy, P.; Goldmann, M.; Bouloussa, O.; Rondelez, F. Spontaneous Chiral Segregation in Bidimensional Films. *Phys. Rev. Lett.* **1995**, *75* (3), 457–460.
- (21) Weissbuch, I.; Berfeld, M.; Bouwman, W.; Kjaer, K.; Als-Nielsen, J.; Lahav, M.; Lieserowitz, L. Separation of Enantiomers and Racemate Formation in Two-Dimensional Crystals at the Water Surface from Racemic α -Amino Acid Amphiphiles: Design and Structure. *J. Am. Chem. Soc.* **1997**, *119*, 933–942.
- (22) Eckhardt, C. J.; Peachey, N. M.; Swanson, D. R.; Takacs, J.; Khan, M. A.; Gong, X.; Kim, J. H.; Wang, J.; Uphaus, R. A. Separation of Chiral Phases in Monolayer Crystals of Racemic Amphiphiles. *Nature* **1993**, *362*, 614–616.
- (23) Zhang, Y. J.; Song, Y.; Zhao, Y.; Li, T. J.; Jiang, L.; Zhu, D. Chiral Discrimination in Langmuir Monolayers of N–Acyl Glutamic Acids Inferred from Π -A Measurements and Atomic Force Microscopy. *Langmuir* **2001**, *17*, 1317–1320.
- (24) Wolfram, S. *Cellular Automata and Complexity – Collected Papers*; Addison-Wesley Publishing Company: Reading, MA, 1994.
- (25) Ladd, S. R. C++ *Simulations and Cellular Automata*; M&T Books: New York, 1995.
- (26) Chopard, B.; Droz, M. *Cellular Automata Modeling of Physical Systems*; Cambridge University Press: Cambridge, UK, 1998.
- (27) Kier, L.; Cheng, C.-K.; Seybold, P. G. Cellular Automata Models of Aqueous Solution Systems. In *Reviews in Computational Chemistry*; Lipkowitz, K. B., Boyd, D. B., Eds.; Wiley: New York, 2001; p 205.
- (28) Testa, B.; Kier, L. B.; Cheng, C.-K. A Cellular Automata Model of Water Structuring by a Chiral Solute. *J. Chem. Inf. Comput. Sci.* **2002**, *42*, 712–716.
- (29) Andelman, D. Chiral Discrimination and Phase Transitions in Langmuir Monolayers. *J. Am. Chem. Soc.* **1989**, *111*, 6536–6544.
- (30) Andelman, D. On the Theory of Tripod Amphiphiles, Chiral Discrimination and Phase Transitions in Langmuir Monolayers. *Physica A* **1990**, *168*, 172–178.
- (31) Andelman, D.; Orland, H. Chiral Discrimination in Solutions and in Langmuir Monolayers. *J. Am. Chem. Soc.* **1993**, *115*, 12322–12329.
- (32) Stine, K. J.; Bono, M. F.; Kretzer, J. S. Observation of a Foam Morphology of the Liquid-Condensed Phase of a Langmuir Monolayer. *J. Coll. Int. Sci.* **1994**, *162*, 320–322.
- (33) Alonso, C.; Artzner, F.; Suchod, B.; Berthault, M.; Kononov, O.; Pécaut, J.; Smilgies, D.; Renault, A. Two- and Three- Dimensional Stacking of Chiral Alcohols. *J. Phys. Chem. B* **2001**, *105*, 12778–12785.
- (34) Uang, J. Y.-J.; Parazak, D. P.; Chui, H. Y.; Stine, K. J. Fluorescence Microscopy Study of Chiral Discrimination in Langmuir Monolayers: Mixed Monolayers of N–Stearoylserine Methyl Ester with Achiral Additives. *J. Coll. Int. Sci.* **1995**, *171*, 366–376.
- (35) Breu, J.; Stoll, A.; Lange, K. G.; Probst, T. Two-Dimensional Diffraction from Enantiopure and Racemic Monolayers of $[\text{Ru}(\text{bpy})_3]^{2+}$ Intercalated into Synthetic Fluorohectorite. *Phys. Chem. Chem. Phys.* **2001**, *3*, 1232–1235.
- (36) Kühnle, A.; Linderth, T. R.; Hammer, B.; Besenbacher, F. Chiral Recognition in Dimerization of Adsorbed Cysteine Observed by Scanning Tunneling Microscopy. *Nature* **2002**, *415*, 891–893.

CI020287E